Journal of Electroceramics, 13, 691–695, 2004

Microstructural Features of RF-sputtered SOFC Anode and Electrolyte Materials

GERARDO JOSE LA O,[1] JOSHUA HERTZ,[1] HARRY TULLER,[1] & YANG SHAO-HORN*,[2]

[1]*Department of Materials Science and Engineering*

[2]*Department of Mechanical Engineering, Massachusetts Institute of Technology, 77 Massachusetts Ave., Cambridge, MA 02139, USA*

Submitted February 13, 2003; Revised February 16, 2004; Accepted February 18, 2004

Abstract. Thin-film samples of yttria-stabilized zirconia (YSZ), nickel oxide (NiO)-YSZ, and YSZ/nickel (Ni)-YSZ bilayer were fabricated by RF-sputtering. The single YSZ layer and YSZ/Ni-YSZ bilayer samples were annealed while the NiO-YSZ layer remained as-deposited. Cross-section transmission electron microscopy (TEM) samples of these thin-films were then prepared, which allowed detailed chemical and structural characterization of these thin-films on the nanometer-scale. Both YSZ and NiO-YSZ layers were fully dense and exhibiting equiaxed grain morphologies. Selected area electron diffraction (SAED) showed the YSZ crystal structure to be predominantly cubic in the annealed samples and amorphous in the as-deposited NiO-YSZ sample. It was found that YSZ film was 70 nm thick and dense, with equiaxed grains ranging from 12–20 nm. Surface roughness of the YSZ in the bilayer fell in the range of 5–20 nm. The Ni-YSZ film in the bilayer was 230 nm thick and porous, which consisted of columnar grains 13–75 nm in length and 9–22 nm in width. The bilayer sample showed no delamination or cracking along the YSZ/Ni-YSZ interface. It is believed that the nano-sized grains, minimal surface roughness and thin layers found in these films are desirable microstructural features for the anode and electrolyte in micro-solid oxide fuel cells (SOFCs). Correlation between microstructural features and electrochemical performance will be reported in a separate study.

Keywords: SOFC, microstructure, transmission electron microscopy, thin-film, sputtering

1. Introduction

Conventional Ni:YSZ/YSZ/$LaSrMnO_3$ solid oxide fuel cells (SOFCs) operate near 1000°C and such high-temperature operation requires the use of costly ceramic interconnects and complex gas seals [1–5]. There have been considerable efforts directed towards cost reduction by lowering the operating temperature to as low as 600°C thereby enabling the use of metal interconnects and simplified gas seals and potentially improving the durability of SOFCs. However, the electrochemical performance of conventional SOFCs at temperatures below 800°C is unsatisfactory; primarily limited by decreased ionic conductivity in the electrolyte [6, 7] and pronounced polarization at the cathode [8, 9]. Fabrication of all thin-film SOFCs would not only allow the miniaturization of conventional SOFCs but also permit the use of thin electrolytes. Electrolyte thickness reduction compensates for reduced ionic conductivity and leads to reasonably high ionic conductance at low temperatures. Previous studies have shown that thin-film electrolytes, from tens of microns to sub-micron thickness range, can be fabricated by chemical vapor deposition [10], spin coating [11, 12], slip casting [13], and sol-gel processing [14], etc. In this study, RF-sputtering was utilized to fabricate thin-film electrolyte layers with thickness on the order of 100 nm. In addition, this method would allow design and fabrication of controlled electrode-electrolyte interface and electrode microstructures and enable systematic studies of oxygen reduction processes at the cathode,

*To whom all correspondence should be addressed. E-mail: shaohorn@mit.edu

essential for progress in reducing cathode polarization at low SOFC operating temperatures.

Microstructural features of thin-film electrolytes and electrodes play an important role in the electrochemical performance of thin-film SOFCs. Ionic conduction in the electrolyte is strongly dependent on crystal structure [15] and grain size [16]. For example, the cubic phase of YSZ exhibits the highest ionic conductivity while nano-sized YSZ grains have been reported to have increased ionic conductivity [17]. Conventional characterization techniques for SOFC electrolyte and electrode materials include scanning electron microscopy (SEM), X-ray diffraction (XRD), AC impedance spectroscopy and optical microscopy. Although they can provide indirect evidence about nano-sized microstructures in thin-film electrolytes and electrodes, transmission electron microscopy (TEM) and associated techniques can give direct structural and chemical information on the nanometer-scale. In this study, we have examined the microstructural features of RF-sputtered thin-film layers of YSZ electrolyte, NiO-YSZ anode precursor, and YSZ/Ni-YSZ bilayer by TEM. Here we report (i) grain size and morphology, (ii) surface roughness, (iii) crystal structure, and (iv) phase distributions in these thin-film layers.

2. Experimental

The YSZ electrolyte film investigated in this study was produced by (1) initially creating a 1 μm low stress silicon nitride (Si_3N_4) layer onto a silicon wafer by chemical vapor deposition (CVD) [18] and (2) depositing YSZ onto the Si_3N_4 top surface by RF-sputtering with plasma power of 2.5 W/cm^2. The RF-sputtered area dimension used in this experiment was 2 cm by 2 cm square. RF-sputtering was performed under a chamber base pressure of approximately 3×10^{-7} Torr and working pressure of 1×10^{-2} Torr with oxygen introduced at a ratio of 9:1 argon to oxygen ensuring complete oxidation of the film. The deposited YSZ film was subsequently annealed in air at 600°C for 1 hour to induce crystallization. Detailed information on the processing of the YSZ film can be found in Ref. [18]. Similar sputtering conditions were used to produce a NiO-YSZ film and a YSZ/Ni-YSZ bilayer. The NiO-YSZ film was produced with nickel being co-sputtered by covering ~25% of the target surface with Ni foil. No heat-treatment was employed on this film. The YSZ/Ni-YSZ bilayer was produced by initially sputtering a NiO-YSZ film onto the Si_3N_4 layer, followed by sputtering a YSZ film onto the NiO-YSZ film. After deposition, the bilayer sample was annealed in reducing atmosphere (5%H_2-95%N_2) at 600°C for 1 hour to reduce the NiO to Ni metal and induce porosity in the anode cermet layer.

TEM samples of these three thin-films were fabricated by initially sectioning the films and substrate into thin cross section, followed by epoxy bonding (*M*-bond 610, Vishray Micro-Measurements) with the sputtered film layers oriented face to face. The resulting composite structure was then mechanically thinned and polished to a thickness of ~10 μm. Thinning to electron transparency was finally performed by ion-milling (Gatan Dual Ion Mill Model 600). Microstructural characterization of the thin-film materials was then performed using a TEM (JOEL 2000FX) operating at 200 keV with a lanthanum hexaboride cathode. Elemental X-ray mapping of Ni and Zr in the YSZ/Ni-YSZ bilayer was also obtained using a scanning transmission electron microscope (HB603 250 keV FEG-STEM) fitted with an Oxford Pentafet energy dispersive X-ray detector (EDS).

3. Results and Discussion

3.1. Microstructure of YSZ Layer

A typical transmission electron micrograph of the YSZ electrolyte film annealed at 600°C and the corresponding selected area electron diffraction (SAED) pattern taken from the area are shown in Fig. 1(a)–(b), respectively. The YSZ film was found dense and composed of equiaxed grains ranging from 6–15 nm with a thickness of approximately 115 nm. SAED analysis revealed the YSZ thin-film to be predominantly cubic ($a =$ 5.139 Å with space group = Fm-3m, JCPDS Card 30-1468), indexed accordingly in Fig. 1(b). The fully dense nature of this RF-sputtered YSZ film makes it desirable as the electrolyte for low-temperature SOFCs. Questions remain regarding the significance of the nano-sized grains on the ionic conductivity [16].

3.2. Microstructure of as-Deposited NiO-YSZ Layer

Figure 2(a) shows a transmission electron micrograph of the as-deposited NiO-YSZ film, which is the

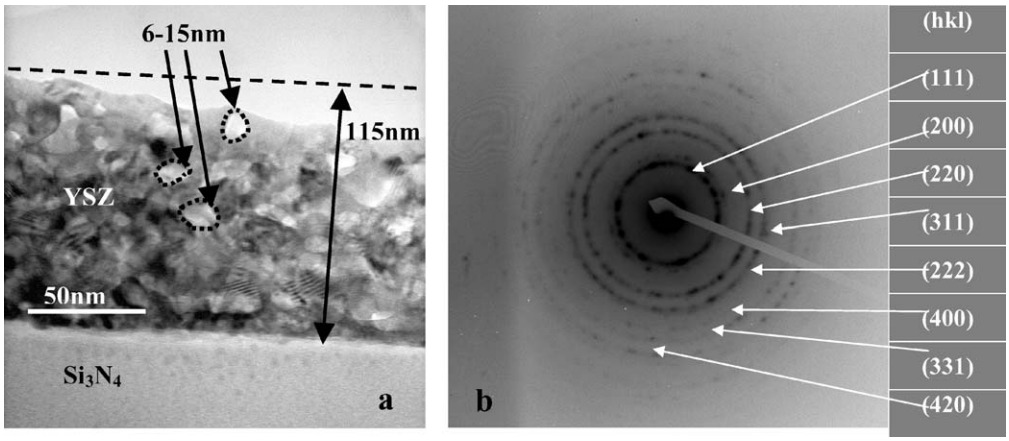

Fig. 1. (a) Transmission electron micrograph of YSZ electrolyte showing dense sputtered film with equiaxed grain sizes measured in the range of 6–15 nm; (b) Indexed polycrystalline electron diffraction pattern from YSZ electrolyte film illustrating predominantly cubic structure with lattice parameter $a = 5.139$ Å and space group = Fm-3m, JCPDS Card 30-1468.

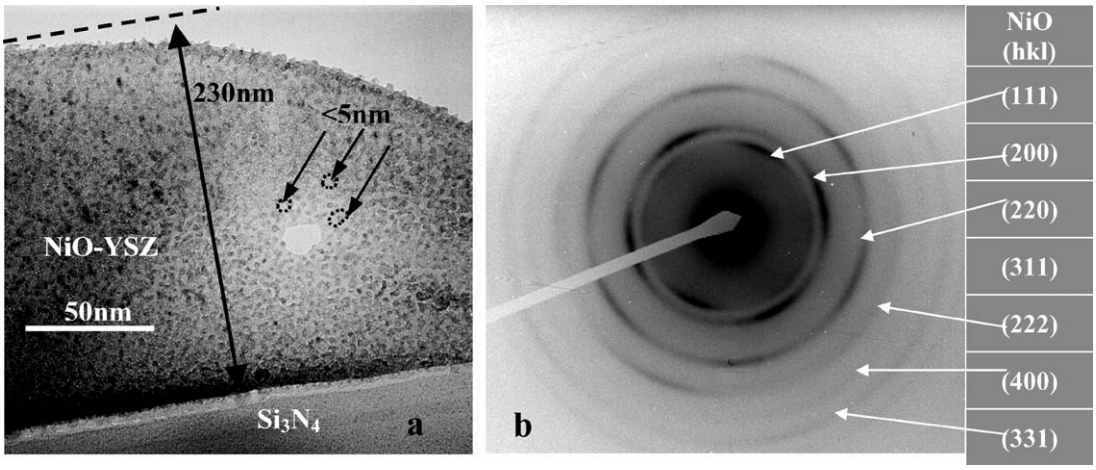

Fig. 2. (a) Transmission electron micrograph of NiO-YSZ layer showing dense film with <5 nm crystallites; (b) Indexed electron diffraction pattern from NiO-YSZ film showing diffraction rings from the NiO phase. The YSZ phase was determined to be amorphous due to the absence of its diffraction rings.

precursor material used to form the Ni-YSZ cermet. The NiO-YSZ film was found fully dense and to have equiaxed grains of less than 5 nm. Electron diffraction analysis revealed the YSZ phase to be amorphous as evidenced by the absence of YSZ diffraction rings in the pattern of NiO-YSZ film, as shown in Fig. 2(b). The NiO phase, on the other hand, was found to be crystalline with predominantly cubic structure ($a = 4.1771$ Å with space group = Fm-3m, JCPDS Card 47-1049) as all the diffraction rings in Fig. 2(b) can be indexed to NiO. The surface of the deposited NiO-YSZ film was also found to be smooth (surface roughness less than 20 nm), making it suitable for bonding to a thin electrolyte layer.

3.3. *Microstructure of YSZ/Ni-YSZ Layer*

A scanning electron micrograph of the YSZ/Ni-YSZ bilayer after annealing in reducing atmosphere

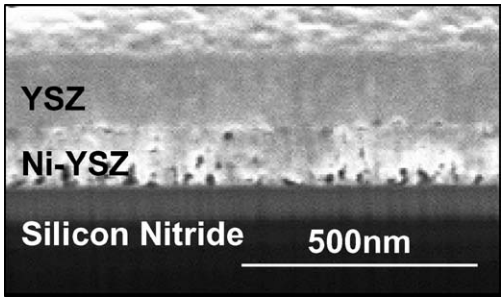

Fig. 3. Scanning electron micrograph of YSZ/Ni-YSZ with pores visible along the Ni-YSZ cermet layer as a result of the decrease in volume upon transformation of NiO to Ni metal during the heat treatment in reducing atmosphere.

(5%H_2-95%N_2) at 600°C for 1 hour is presented in Fig. 3. Pores along the Ni-YSZ film, formed upon the reduction of NiO to Ni metal, are readily observable. A transmission electron micrograph from this YSZ/Ni-YSZ sample and the corresponding SAED taken from the area are shown in Figs. 4(a)–(b), respectively. The YSZ film was found to have a thickness of approximately 70 nm and the Ni-YSZ film to be roughly 250 nm thick. It should be noted that the YSZ film is fully dense with equiaxed grains in the range of 12–20 nm while the Ni-YSZ cermet is porous with columnar grains measuring 13–75 nm in length and 9–22 nm wide. The electron diffraction pattern in Fig. 4(b) revealed that the YSZ/Ni-YSZ bilayer consisted of polycrystalline Ni and YSZ. High-resolution transmission electron microscopy studies are needed to further resolve individual grains of Ni and YSZ in the bilayer. Similar to the annealed YSZ single layer, the YSZ phase was predominantly cubic ($a = 5.139$ Å with space group = Fm-3m, JCPDS Card 30-1468). The surface roughness of the YSZ film was determined to range from 5–20 nm. It is believed that this bilayer structure possesses the desired nano-sized grains in the anode that can provide for high surface area Ni and leading to increased triple phase boundaries (TPBs) and thus reduced anodic overpotential. In addition, the layers show no delamination or cracking along the bilayer interface, desirable for decreased contact resistance in the SOFC.

Preliminary results from X-ray mapping on the YSZ/Ni-YSZ layer are shown in Fig. 5, in which Zr is highlighted in white (Fig. 5(a)) and Ni is highlighted in white (Fig. 5(b)). It is shown clearly that Ni was only detected in the Ni-YSZ anode cermet and was absent in the YSZ layer. The black regions constitute areas with no presence of the detected element while the "fingerprint" patterns on the image result from an artifact in the X-ray mapping software. Although these results have shown a clear separation between the anode-cermet and electrolyte layers, Ni-rich regions are not resolved in the Ni-YSZ anode cermet. Further improvements on resolution of this technique and application of electron energy loss spectroscopy are required in order to quantify the extent and morphology of the individual Ni grains.

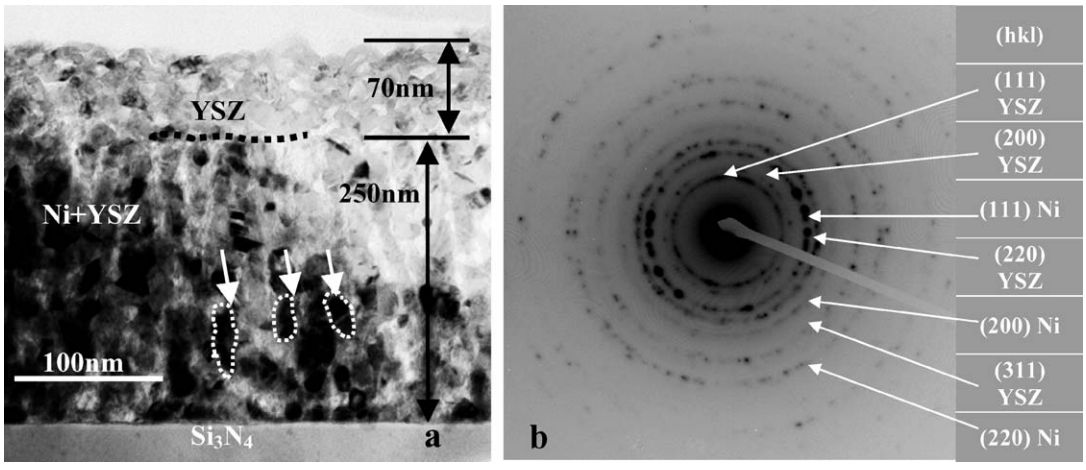

Fig. 4. (a) Transmission electron micrograph of YSZ/Ni-YSZ bilayer showing 70 nm dense YSZ layer and 250 nm columnar grained Ni-YSZ; (b) Indexed electron diffraction pattern showing polycrystalline Ni and YSZ phases in the bilayer.

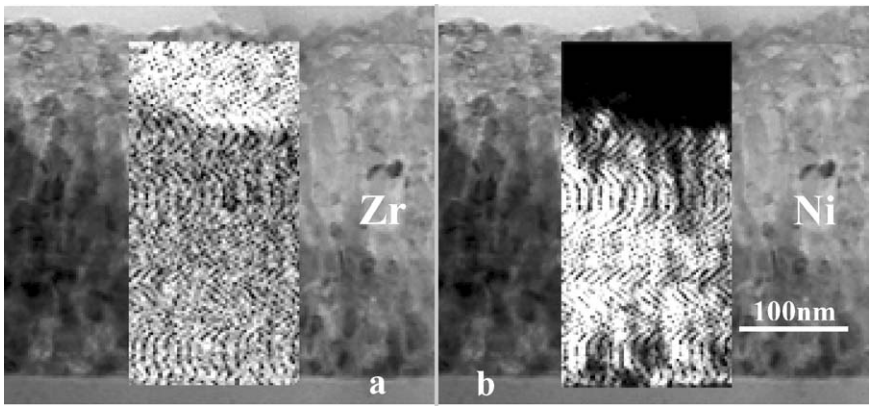

Fig. 5. Results from X-ray mapping on YSZ/Ni-YSZ bilayer with (a) Zr and (b) Ni rich areas highlighted. A clear separation between the electrolyte and cermet-anode layers is observed. "Fingerprint" like patterns on the image constitute a malfunction in the X-ray mapping software.

4. Conclusions

Dense YSZ electrolyte films with nano-sized grains and thickness on the order of 100 nm and a bilayer structure of dense YSZ electrolyte and porous Ni-YSZ cermet with good adhesion between the layers have been successfully fabricated. TEM characterziation of thin-film YSZ and Ni-YSZ layers has allowed a detailed examination of microstructural features important to ionic conduction and electrocatalytic processes. This enables correlation of microstructural features with processing parameters and eventually electrochemical performance of thin-film SOFCs.

Acknowledgments

This work was supported by the FORD-MIT Alliance and the DoD Multidisciplinary University Research Initiative (MURI) program under Grant DAAD19-01-1-0566.

References

1. N.Q. Minh, *Journal of the American Ceramic Society*, **76**, 563 (1993).
2. T. Schwickert, R. Sievering, P. Geasee, and R. Conradt, *Materialwissenschaft Und Werkstofftechnik*, **33**, 363 (2002).
3. K.Q. Huang, P.Y. Hou, and J.B. Goodenough, *Solid State Ionics*, **129**, 237 (2000).
4. S.P. Simner and J.W. Stevenson, *Journal of Power Sources*, **102**, 310 (2001).
5. S.C. Singhal, *Solid State Ionics*, **135**, 305 (2000).
6. T. Fukui, S. Ohara, K. Murata, H. Yoshida, K. Miura, and T. Inagaki, *Journal of Power Sources*, **106**, 142 (2002).
7. J.M. Ralph, A.C. Schoeler, and M. Krumpelt, *Journal of Materials Science*, **36**, 1161 (2001).
8. T. Tsai and S.A. Barnett, *Solid State Ionics*, **93**, 207 (1997).
9. N.Q. Minh, in *Conference Presentation in Materials for Fuel Cells and Fuel Processors Symposium* (MRS Fall Meeting, Boston, December 2002).
10. M. Balog, M. Shieber, M. Jichiman, and S. Patai, *J. Electrochem. Soc.*, **126**, 1203 (1979)
11. C.C. Chen, M.M. Nasrallah, and H.U. Anderson, *Solid State Ionics*, **70**, 101 (1994).
12. T. Hibino, A. Hashimoto, K. Asano, M. Yano, M. Suzuki, and M. Sano, *Electrochemical and Solid State Letters*, **5**, A242 (2002).
13. S. deSouza, S.J. Visco, and L.C. DeJonghe, *Solid State Ionics*, **98**, 57 (1997).
14. K. Mehta, R. Xu, and A.V. Virkar, *Journal of Sol-Gel Science and Technology*, **11**, 203 (1998).
15. I.R. Gibson, G.P. Dransfield, and J.T.S. Irvine, *Journal of the European Ceramic Society*, **18**, 661 (1998).
16. H.L. Tuller, *Solid State Ionics*, **131**, 143 (2000).
17. I. Kosacki, B. Gorman, and H.U. Anderson, in *Ionic and Mixed Conductors*, edited by T.A. Ramanarayanan, W.L. Worrell, H.L. Tuller, A.C. Kandkar, M. Mogensen, and W. Gopel (The Electrochemical Society, Pennington, NJ, 1998), p. 631.
18. J.L. Hertz, J. Lappalainen, and H.L. Tuller, in *Conference Presentation in Materials for Fuel Cells and Fuel Processors Symposium*, (Boston, MRS Fall Meeting Dec. 2002).